



A Green Method for Preparation of Amino Acids Functionalized 2,3-Dialdehyde Cellulose

Atef Kalmouch¹, Mohamed El-Sakhawy^{*2}, Samir Kamel², Ahmed Salama² and Peter Hesemann³

¹Peptide Chemistry Department, National Research Centre, 33, El-Bohouth Str., P.O. 12622, Dokki, Giza, Egypt.

²Cellulose and Paper Department, National Research Centre, 33 El Bohouth Str., P.O. 12622, Dokki Giza, Egypt.

³Institut Charles Gerhardt, UMR 5253 CNRS-UM-ENSCM, CMOS, Université de Montpellier, Place Eugène Bataillon, 34095 Montpellier Cedex 05, France.



CrossMark

THIS study depicts the preparation of a new amino cellulose derivative of cellulose extracted from bagasse. 2,3-dialdehyde cellulose (DAC) with 60% degree of oxidation was prepared from cellulose by periodate oxidation. The obtained DAC was functionalized by Schiff base reaction with several amino acids up to 2.55% nitrogen content. Aliphatic/Aromatic, Mono/Dibasic, and Mono carboxylic/Dicarboxylic amino acids were investigated for the Schiff base reaction. FTIR spectra confirmed the successful introduction of the amino acids functional groups (carboxyl and amino groups). The successful interaction of amino acids with DAC composites were characterized and confirmed by elemental analysis, EDAX, TEM, SEM, XRD and TGA. A green method for preparation of amino acids functionalized 2,3-dialdehyde cellulose could be obtained in an efficient manner by controlling the amino acid type and degree of substitution while producing the DAC composites.

Keywords: Cellulose reaction; Periodate oxidation; 2,3-dialdehyde cellulose; Amino acid.

Introduction

Cellulose is an attractive promising candidate biopolymer since it is the most abundant organic raw materials on the world and available from various sources [1]. It is biodegradable, renewable, biocompatible and inexpensive [2]. Nevertheless, cellulose bioactivity towards different vital applications is limited due to the presence of only hydroxyl groups as functional groups on the cellulose fibers outer layer [3]. To enhance cellulose activity some studies have been reported such as blending with bioactive polymers [4] or grafting with functional monomers or amino acids [5].

Recently periodate oxidation of cellulose

have been reported as a simplistic process for cellulose functionalization [6]. Specific cleavage of cellulose C2-C3 bond provides dialdehyde cellulose which can act as a reactive intermediate for further chemical reactions [7]. DAC with different degrees of oxidation could be prepared by periodate oxidation and were further undergo Schiff base formation via reductive amination with amine containing materials such as amino acids in a simple procedure [8]. Periodate oxidation provides a high density of negative charges on cellulose surface from introduced carboxylate groups, which force the adsorption of biomolecules [5]. Amino acids possess different polar functional groups; for instance amine, hydroxyl and carboxyl groups [9]. The obtained

*Corresponding author e-mail: elsakhawy@yahoo.com

Received 16/1/2020; Accepted 2/3/2020

DOI: 10.21608/ejchem.2020.22552.2341

© 2020 National Information and Documentation Center (NIDOC)

Schiff bases were used for different applications for instance sensors [10], oil-water stabilizer [11], biomaterials [12, 13] and metal removal [14].

Various compounds containing amine such as amino acids, antibiotics and enzymes could be applied to cellulose via periodate oxidation followed by reductive-amination for potential biomedical applications [15]. Schiff-base formation could be a concept for Congo red removal via reacting due with crosslinked DAC [16]. Amino-functionalized cellulose was proven as an efficient adsorbent for anionic dyes [17], while DAC modified with Polyethylenimine (PEI) was used successfully for Cu (II) removal [18]. Amino-functionalized cellulose nanocrystals/chitosan composite have been designed to remove harmful residual diclofenac sodium to save the environment [19]. Antibacterial biomaterials have been prepared from chitosan biopolymer Schiff base by coupling with isatin under acidic conditions [20].

The aim of the present study is to use sustainable cellulose to attain an environmentally friendly nature biomaterial which could be applicable for biomedical and environmental applications. Cellulose was firstly extracted from bagasse and subjected to oxidation by sodium periodate to attain C-2/C-3 dialdehyde cellulose (DAC). Oxidized cellulose has been reacted with amino acids to comprise amino acids onto the surface of cellulose dialdehyde through a reductive-amination treatment, and then evaluate the reaction efficiency.

Materials and Method

Raw material

The raw material used in this work is sugar cane bagasse, delivered from Quena Company of Paper Industry, Egypt.

Extraction of cellulose from sugar cane bagasse

The manufacture of cellulose involves several reaction steps. Sugar cane bagasse was hydrolyzed with 1.5% HCl, based on the raw

material, using liquor ratio of 1:10 at 120°C for 2h. The prehydrolyzed bagasse was treated with 20% NaOH using liquor ratio of 1:7 at 170°C for 2h giving unbleached bagasse pulp. The treated bagasse was bleached by sodium chlorite to remove the residual lignin. The chemical analysis of the produced pulp is (α -Cellulose 94.2%, Lignin 0.3%, Hemi-cellulose 3.4%, and Ash 0.4%)

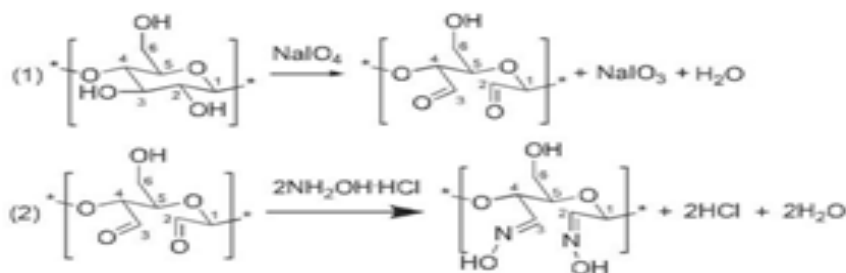
Oxidation of Cellulose

DAC was synthesized according to the procedure described by Sirvio with little modification [21]. In brief, DAC was prepared by oxidizing 1 g of cellulose using 0.8 g of sodium periodate as an oxidant in 50 ml distilled water and a reaction vessel was covered with an aluminum foil to prevent the photo-induced decomposition of periodate. The reaction mixture was stirred with a magnetic stirrer in a water bath at 70°C for 3h. After washing with deionized water (3 portions, about 2000 ml), DAC was stored in a non-dried state at 4°C.

Determination of the aldehyde content by titration method

The determination of aldehyde contents of DAC, degree of oxidation (D.O.), was based on oxime reaction between aldehyde group and the hydroxyl amine hydrochloride (NH₂OH.HCl). The non-dried DAC (0.1 g) was mixed with 25 ml of 0.25 M NH₂OH.HCl and stirred in a 250 ml beaker covered with aluminum foil for 48h at room temperature. Product was filtrated and washed with deionized water after which it was dried in a freeze-dryer.

0.25 M hydroxylamine hydrochloride-solution was prepared by first dissolving 17.55 g hydroxyl amine hydrochloride (99%) in 150 ml of water. The solution was then diluted to 1 liter and pH was adjusted to 4.0 with 0.1 M NaOH. The hydroxylamine hydrochloride reacts with aldehyde group to generate hydrochloric acid. The aldehyde content of oxidized DAC can be determined by sodium hydroxide titration of the released hydrochloric acid [22].



equation 1

According to equation 1, one mol of aldehyde reacts with one mol of $\text{NH}_2\text{OH}\cdot\text{HCl}$. A DAC solution with the same concentration at a pH of 5 was used as a blank, and its consumption of the alkali solution in ml was recorded as V_{control} . So, the degree of oxidation can be calculated from the equation 2:

$$\text{DO}\% = \left[\frac{M_{\text{NaOH}} (V_{\text{sample}} - V_{\text{control}})}{m/M_w} * 100 \right] \quad \text{equation 2}$$

where M_{NaOH} is 0.1 M, m is the dry weight of the DAC sample (g), and M_w is the molecular weight of the repeating unit, $(\text{C}_6\text{H}_8\text{O}_{10})_n$, in DAC (160.124 g/mol).

Reaction of dialdehyde cellulose with amino acids

The dibasic amino acids namely aspartic and glutamic were added to the DAC suspended in methanol followed by one equivalent of triethylamine (TEA) as a catalyst and then were stirred for 6 hrs at 30°C . On the other hand, other amino acids, lysine, β -alanine, phenylalanine, and p -amino benzoic acid were stirred with suspended DAC without catalyst. The color of the reaction medium changes from bright white to yellowish to brown during the reaction time referring to the imine group or the Schiff base formation. When no physical change had been observed the mixture is refluxed for 4-8 h, filtered, washed with MeOH and generally air dried in desiccator. Amino acid was added in a ratio of 1.5 equivalents to DAC. During the reaction, one of the amine groups reacts with the aldehyde group of DAC to generate an imine bond, while the other one remains as a free primary amine.

Characterization

Elemental Analysis

The mass ratios of C, H, O and N of each sample were measured using Elemental Analyzer Vario EL III Elementar (Langensfeld, Germany). Measurements were done at least in duplicate.

Fourier Transform Infrared Spectroscopy

Fourier transform infrared (FTIR) spectra of cellulose, DAC, and amino acids functionalized dialdehyde cellulose were recorded with a FTIR spectrometer (Nicolet Impact-400 FT-IR spectrophotometer) in the range of 200– 4000 cm^{-1} .

XRD

The XRD patterns investigations of cellulose and DAC were measured by using an Empyrean Powder Diffractometer (Shimadzu, Japan). The diffraction patterns were determined with a scanning angle 2θ ranging from 4° to 50° in step scan intervals of 0.02° , with Cu $K\alpha$ radiation ($k = 1.5418 \text{ \AA}$) at 40 kV and 40 mA.

Transmittance electron microscopy (TEM)

The particle size of DAC was measured using transmittance electron microscopy, (JSM 6360LV, JEOL/Noran) operated at 200 kV.

Scanning electron microscopy (SEM)

SEM was done on a JEOL JXA-840A Electron probe microanalyzer with tungsten filament (30 kV).

EDX

The elemental composition of the composite surface was evaluated by using an energy dispersive X-ray spectroscopy (EDX) detector, Oxford INCAx-sight SN with a resolution of 128 eV at 5.9 keV, attached to the Hitachi S-4700 SEM.

Thermo gravimetric analysis

The thermal stability of cellulose, DAC, and amino acids functionalized dialdehyde cellulose was tested by thermogravimetric analysis (TGA, Shimadzu DTG-60, Japan) at a heating rate of $10^\circ\text{C}/\text{min}$ from 25 to 800°C under a nitrogen atmosphere in order to avoid thermo-oxidative reactions.

Solid state Nuclear magnetic resonance spectrometry (NMR) spectroscopy

^{13}C Cross Polarization Magic Angle Spinning (CP/MAS) spectra were recorded at room temperature on a Varian VNMRs 400 MHz spectrometer operating at 100.5 MHz using a two-channel probe with 3.2 mm ZrO_2 rotors.

Results and Discussion

Oxidation of Cellulose

Conversion of cellulose to the dialdehyde cellulose was carried out by periodate oxidation. It is a famous reaction that leads to the formation of DAC by opening the anhydrous glucose unit (AGU) of cellulose by selective cleavage of diol at 2, 3 position yielding the 2,3-dialdehyde cellulose groups. The periodate anion gives a cyclic intermediate through the co-ordination with 2,3-diol. Such intermediate rapidly converts to the dialdehyde by the loss of iodate. According to the

equilibrium reaction equation, one mole of NaIO_4 reacted with one mole of AGU to form two moles of aldehyde groups. Periodate could be recovered after oxidation, but an excess of periodate should be used to accomplish satisfactory oxidation level [23].

The oxidation reaction was carried out in aqueous medium and the DAC dispersion was precipitated in heterogeneous medium (3:1 t-butyl alcohol: water). Even after complete oxidation, the oxidized DAC is not soluble in water or common organic solvents. This insolubility was referred to the hemiacetal formed between aldehyde groups with residual hydroxyl groups of DAC. However, complete solubilization of raw DAC can be reached by the prolonged heating in water process to disturb the formed hemiacetals [24].

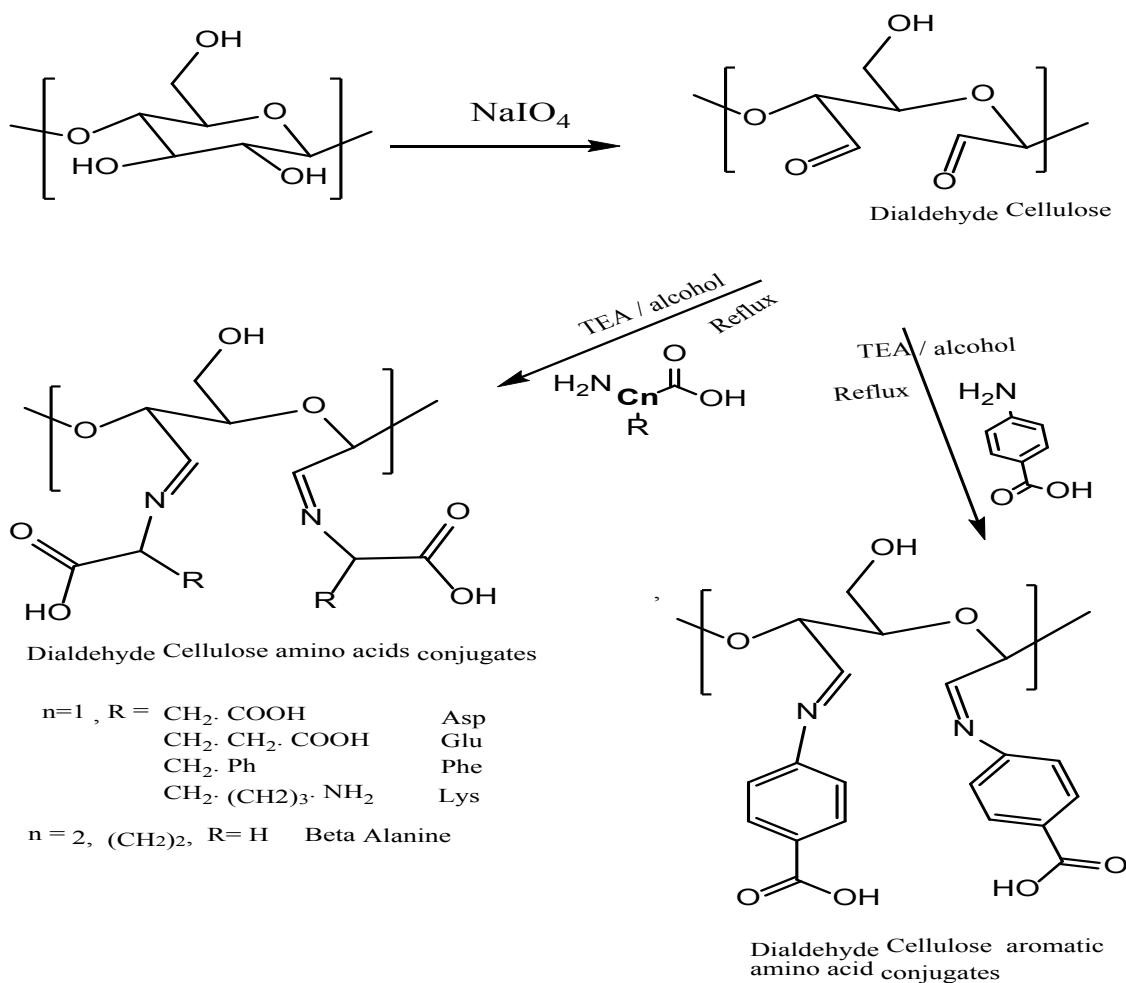
In our work, degree of cellulose oxidation was 60% (aldehyde content). The degree of

oxidation can be readily controlled. Depending on the quantity of periodates employed, DAC is available in oxidation level varies from 0 to 100%. The high aldehydes group proportion in the DAC chain confirms the superior oxidation level and cellulose reactivity.

Reaction of Dialdehyde Cellulose with Amino Acids

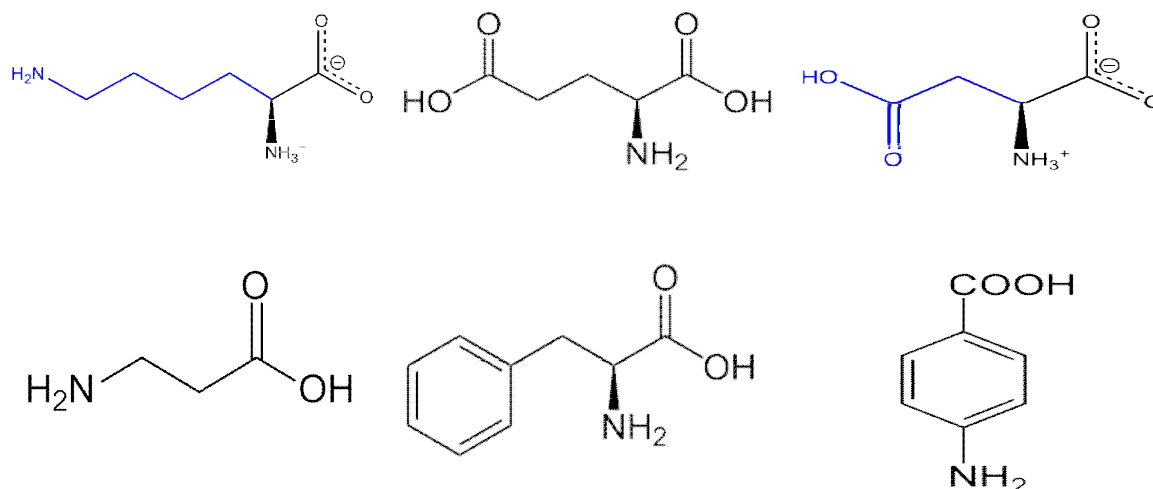
The obtained aldehyde groups, obtained after cellulose oxidation, have superior reactivity towards extra modification than their parent hydroxyl groups. Subsequently the resulting active aldehyde groups in the oxidized cellulose could be modified with amino groups of amino acid to form the covalent imine bonding of Schiff base and successfully obtained the DAC amino acid derivatives.

Scheme 1 illustrates the periodate oxidation of cellulose to DAC and its reaction with aliphatic and aromatic amino acids.



Scheme 1. Preparation of Dialdehyde Cellulose amino acids conjugates.

The structures of amino acids that used in this study are the following:



Degree of substitution by amino acids

The degree of substitution of 2,3-dialdehyde cellulose by amino acids has been estimated from elemental analyses of the prepared samples (Table 1) using the following equation:

$$DS = \frac{MWt(\text{cellulose, dialdehyde, starch ..}) * N\%}{[100 * 14 - (N\% * MWt \text{ of nitrogen containing agent})]}$$

equation 3

$$DS = \frac{196 * N\%}{1400 - (N\% * \text{amino acid M Wt})}$$

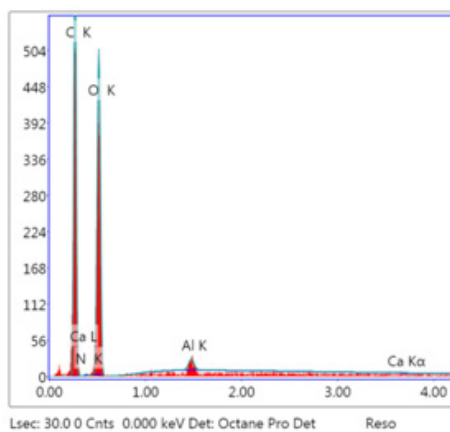
equation 4

EDX analysis was carried out to investigate the C, O, and N content of the prepared DAC amino derivatives (Figure 1). Results were depicted in the Table 1 compared with that of elemental analysis.

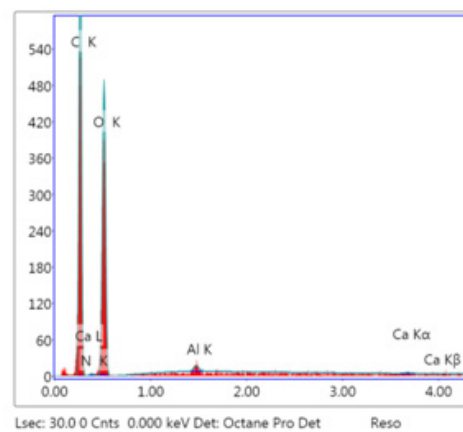
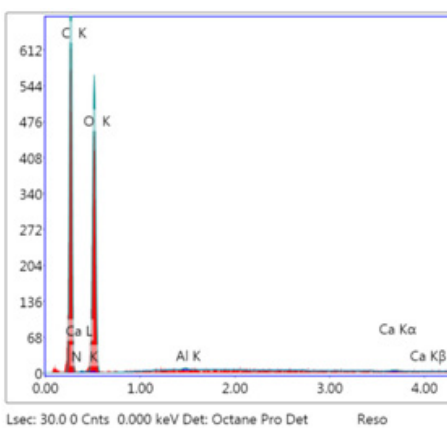
Results show that only 3–10% of the aldehyde groups were converted to amino acid derivative. The low reaction effectiveness could be due to the low rate of imine formation in the aqueous environment [25]

TABLE 1. Elemental analysis of amino acids functionalized 2,3-dialdehyde cellulose.

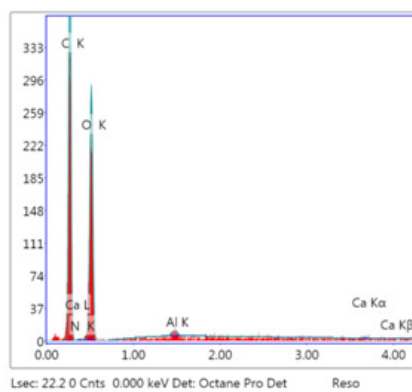
Name	M. Wt.	C %	H %	O %	N %	DS
Phenylalanine (EA) (EDAX)	165	43.14	5.944		0.416	0.061
		49.23		49.31	1.05	0.168
B- alanine (EA) (EDAX)	89	42.20	6.216	-	0.757	0.111
		47.2	-	51.11	1.5	0.232
Lysine (EA)	146	43.89	6.326	-	2.547	0.207
		44.17	6.086	-	0.823	0.125
4-aminobenzoic (EA) (EDAX)	137	47.19	-	51.06	1.37	0.221
Glutamic acid (EA) (EDAX)	147	43.06	6.05	-	1.28	0.207
		47.03	-	51.71	0.7	0.152
Aspartic acid (EA) (EDAX)	133	43.18	6.30	-	0.43	0.063
		47.93	-	50.38	1.29	0.206



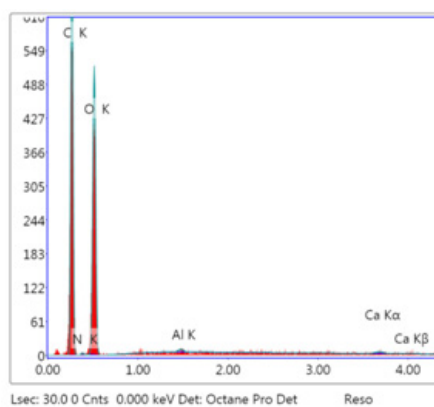
Glutamic acid



Aspartic acid



Phenylalanine

 β -Alanine

p-Aminobenzoic acid

Fig. 1. EDX of the DAC amino acids derivatives .

FTIR of cellulose and DAC

TABLE 2. Characteristic Bands of Cellulose [26].

Wavenumber (cm ⁻¹)	Assignment
3482.81	A strong hydrogen- bonded O-H stretching vibration.
2897.52	C-H stretching.
1645.95	O-H bending from absorbed water.
1428.99	CH ₂ bending of pyran ring Or C-O stretching of the syringe ring of lignin & aromatic skeletal vibration of lignin.
1034.62	C-O-C pyranose ring vibration
898.666	β -Glycosidic linkage between glucose units in cellulose.
662.428	O-H out of plane bending.

TABLE 3. Characteristic Bands of DAC.

Wavenumber (cm ⁻¹)	Assignment
3431.71	hydrogen bonded O-H stretching
2937.06	sp ³ hybridized C-H stretching.
1743.41	C=O stretching of aldehyde groups
1088.62	Indicates the presence of hemiacetal.

Figure 2 and Tables 2 & 3 show the characteristic FTIR peaks for cellulose and DAC. These results showed that the hydroxyl groups on the DAC molecular chain were partly oxidized to aldehyde groups, producing the dialdehyde cellulose as evident from the C=O band for DAC at 1743 cm⁻¹.

The amino group of amino acids reacts with aldehyde groups of oxidized cellulose molecules to produce Schiff base, so carbonyl group (H-C=O) which usually has an absorbance band of stretching at 1740-1720 cm⁻¹ was disappeared and a new azomethine (-C=N-) group stretching absorption band at 1690-1640 cm⁻¹ appeared (Figure 3).

FTIR spectrum of Lysine amino acids Schiff base (Figure 3a) with oxidized cellulose dialdehyde shows a broad strong stretching vibration band at 3346.85 cm⁻¹ for (OH) hydrogen bonded with (OH) stretching of moisture molecule and N-H of the amino group. In addition, medium stretching vibration at 2904.24 cm⁻¹ due to (CH) of (CH₂) groups of the aliphatic chain. Also, a stretching

vibration band at 1631.48 cm⁻¹, due to (-N=C) or imine group formed from the condensation reaction, a weak bending and rocking vibration band at 1369.21 (COO-) bending vibration [27]. Bending vibration band at 1340.64 cm⁻¹ due to (H-C of CH₂-C=O) group and stretching band at 1158 cm⁻¹ due to C-N group. Finally, strong stretching band at 1060 cm⁻¹ is due to (C-O-C) of cellulose structure [28].

The FTIR spectrum of both Glutamic and Aspartic acids Schiff's bases (Figure 3b & c) show medium broad absorption band at 3412 cm⁻¹ for (OH) hydrogen bonded with (OH) stretching of moisture molecule and a stretching vibration band at 3115.44 cm⁻¹ due to (OH) of (COOH) groups overlay forming the broad band. In addition, spectrum show medium stretching vibration at 2922.59 cm⁻¹ due to (CH) of (CH₂) groups of the aliphatic chain, and small stretches vibration at 2655.5 cm⁻¹ due to (OH) of the COOH group. Also, a weak stretching vibration band at 1686.44 cm⁻¹ due to (C=O of the COOH) group and at 1586.16 cm⁻¹ (asym.), 1374 (sym.) cm⁻¹ due to (COO-) bending vibration is shown. Figures

show a bending vibration band at 1455.03 cm^{-1} due to (H-C of CH_2) group and stretching band at 1160.96 cm^{-1} due to C-N group. Finally, strong

stretching band at 1021.12 cm^{-1} is due to (C-O-C) of cellulose structure [27, 28].

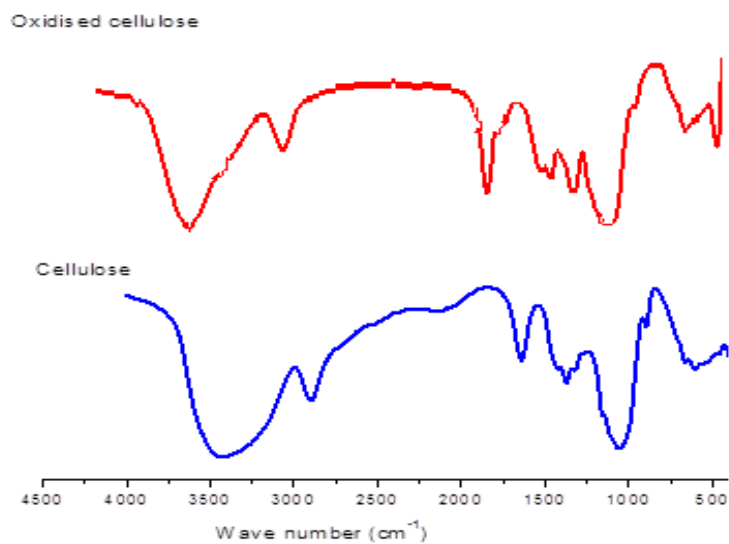


Fig. 2. FTIR of cellulose and DAC.

FTIR Study for amino acids functionalized DAC

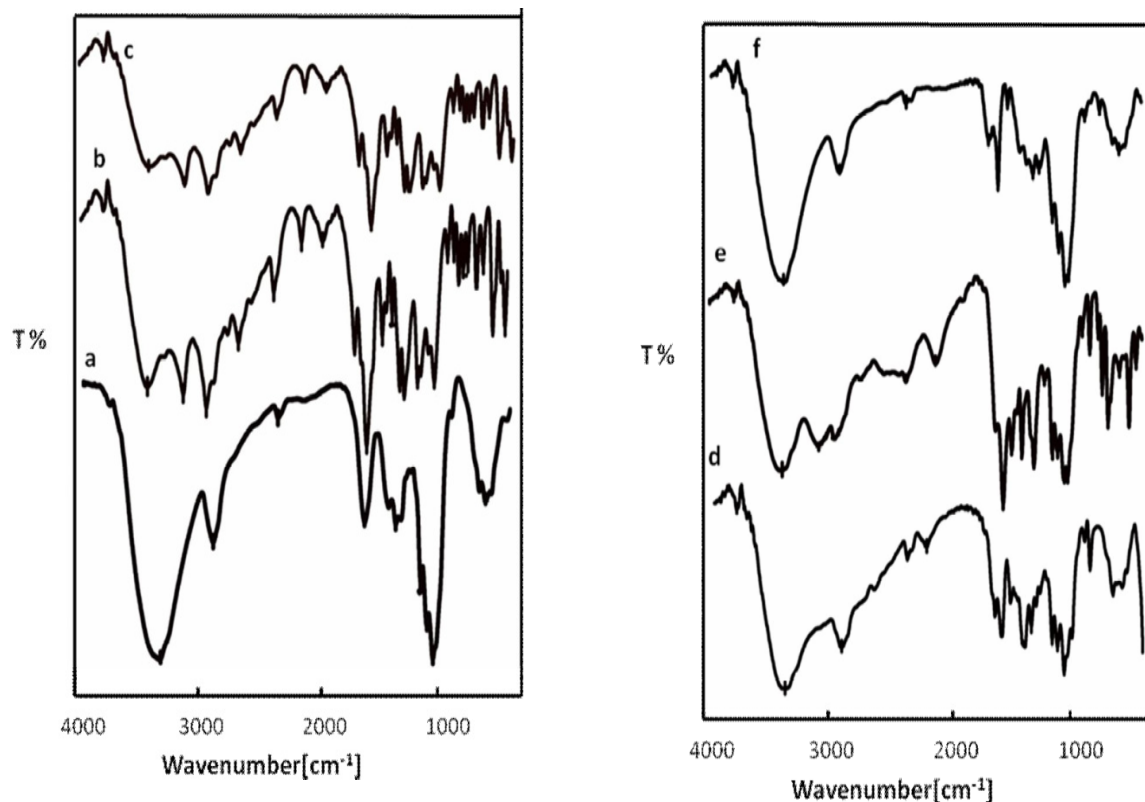


Fig. 3. FTIR spectra of amino acids-cellulose derivatives; a) Lysine, b) Glutamic acid, c) Aspartic acid, d) β -Alanine, e) Phenylalanine, f) *p*-Aminobenzoic acid.

The FTIR spectrum of β -Alanine Schiff's base (Figure 3d) with oxidized cellulose dialdehyde shows a broad strong stretching vibration band at 3380.6 cm^{-1} for (OH) hydrogen bonded with (OH) stretching of moisture molecule. In addition, medium stretching vibration at 2909.1 cm^{-1} due to (CH) of (CH₂) groups of the aliphatic chain, small stretches vibration at 2655.5 cm^{-1} due to (OH) of the COOH group. Also, a weak stretching vibration band at 1634.38 cm^{-1} , due to (-N=C) or imine group formed from the condensation reaction, a weak stretching vibration band at 1578.45 cm^{-1} due to (C=O of the COOH) group and at 1330.64 cm^{-1} (COO-) bending vibration. Bending vibration band at 1384.64 cm^{-1} due to (H-C of CH₂-C=O) group and stretching band at 1158 cm^{-1} due to C-N group. Finally, strong stretching band at 1057.76 cm^{-1} is due to (C-O-C) of cellulose structure.

The FTIR spectrum of Phenylalanine Schiff's base (Figure 3e) with oxidized cellulose dialdehyde, shows a broad strong stretching vibration band at 3383.5 cm^{-1} for (OH) hydrogen bonded with (OH) stretching of moisture molecule and a stretching vibration band at 3082.65 cm^{-1} due to (OH) of (COOH) groups. In addition medium stretching vibration at 2954.41 cm^{-1} is due to (CH) of aromatic ring. Also the figure shows a weak stretching vibration band at 1640 cm^{-1} , due to (-N=C) or imine group formed from the condensation reaction, a stretching vibration band at 1562.06 cm^{-1} due to (C=O of the COOH) group and at $1439.64, 1309.43\text{ cm}^{-1}$ for (C-O of COO-) bending vibration. Bending vibration band at 1408.75 cm^{-1} due to (C=C of aromatic

ring) and $745.35, 697.14\text{ cm}^{-1}$ for C-H aromatic out of plane bending vibration is shown. Band at 1156 cm^{-1} is due to C-N group and finally, strong stretching band at 1030.77 cm^{-1} is due to (C-O-C) of cellulose structure.

The FTIR spectrum of p-aminobenzoic acid Schiff's base (Figure 3f) with oxidized cellulose dialdehyde, shows a broad strong stretching vibration band at 3366.14 cm^{-1} for (OH) hydrogen bonded of COOH. In addition medium stretching vibration at 2906.2 cm^{-1} is due to (CH) of aromatic ring. Also, figure shows a weak stretching vibration band at 1685.48 cm^{-1} , due to (-N=C) or imine group formed from the condensation reaction, and band at 1606.41 cm^{-1} due to (C=O of the COOH) group and at $1320.04, 1159.97\text{ cm}^{-1}$ for (C-O of COO-) bending vibration. Bending vibration band at 1529.27 cm^{-1} is due to (C=C of aromatic ring) and while band at 897.7 and 772.35 cm^{-1} C-H is due to aromatic out of plane bending vibration. Figure shows band and at 1056.8 cm^{-1} due to C-N group and finally, stretching band at 1027.87 cm^{-1} due to (C-O-C) of cellulose structure [27, 28].

Transmission electron microscopy (TEM) was used for investigating the internal shape of DAC. Figure 4 shows the formation of particles of average 94.3 nm . Individualized crystallinities of rod-like shape with some aggregate or non-disintegrated fibrils were also observed.

SEM is one of the most important tools used for observing microstructure and surface morphology of the synthesized product. SEM micrographs of functionalized derivatives are shown in Fig. 5.

TEM & SEM of DAC amino acids derivatives

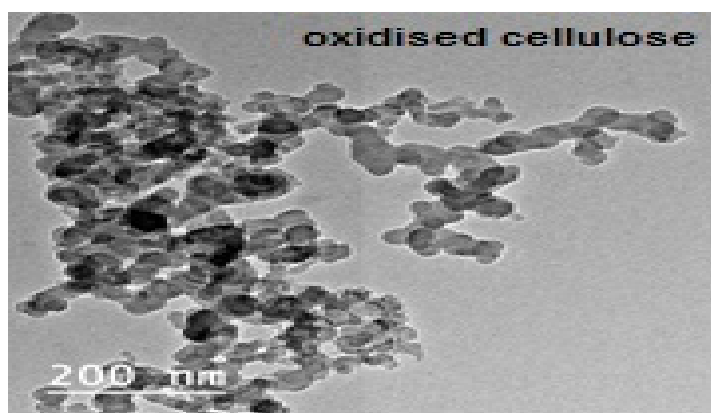


Fig. 4. TEM of DAC.

The SEM images of cellulose (Fig. 5) show the heterogeneous rough surface and highly aggregated fibers with sheet-like morphology with an average diameter of 10–30 μm and a length of 100–200 μm .

As previously described, extensive periodate oxidation, causes a drastic change to the morphology of cellulose (since, it leads to the formation of beads with a relatively smooth surface). Oxidized DAC by NaIO_4 have a high aspect ratio with micro porous structure and large specific surface area. After oxidation fibrils became thicker and also showed a rough and slightly curved character and no obvious proof for phase-separated structure was observed.

The morphology of DAC amino derivatives seems to be homogenous without phase-separated structure. Furthermore, the reductive amination with different investigated amino acids on DAC provided uniform rod-like crystallinities materials with less compact and more porous texture, which increased specific surface area. Some non-collapsed fibrils were also observed, particularly in the case of p-aminobenzoic acid. However, the surface of modified DAC looks smoother and agglomerated due to the chemical modification and resultant new association with the different aldehyde groups.

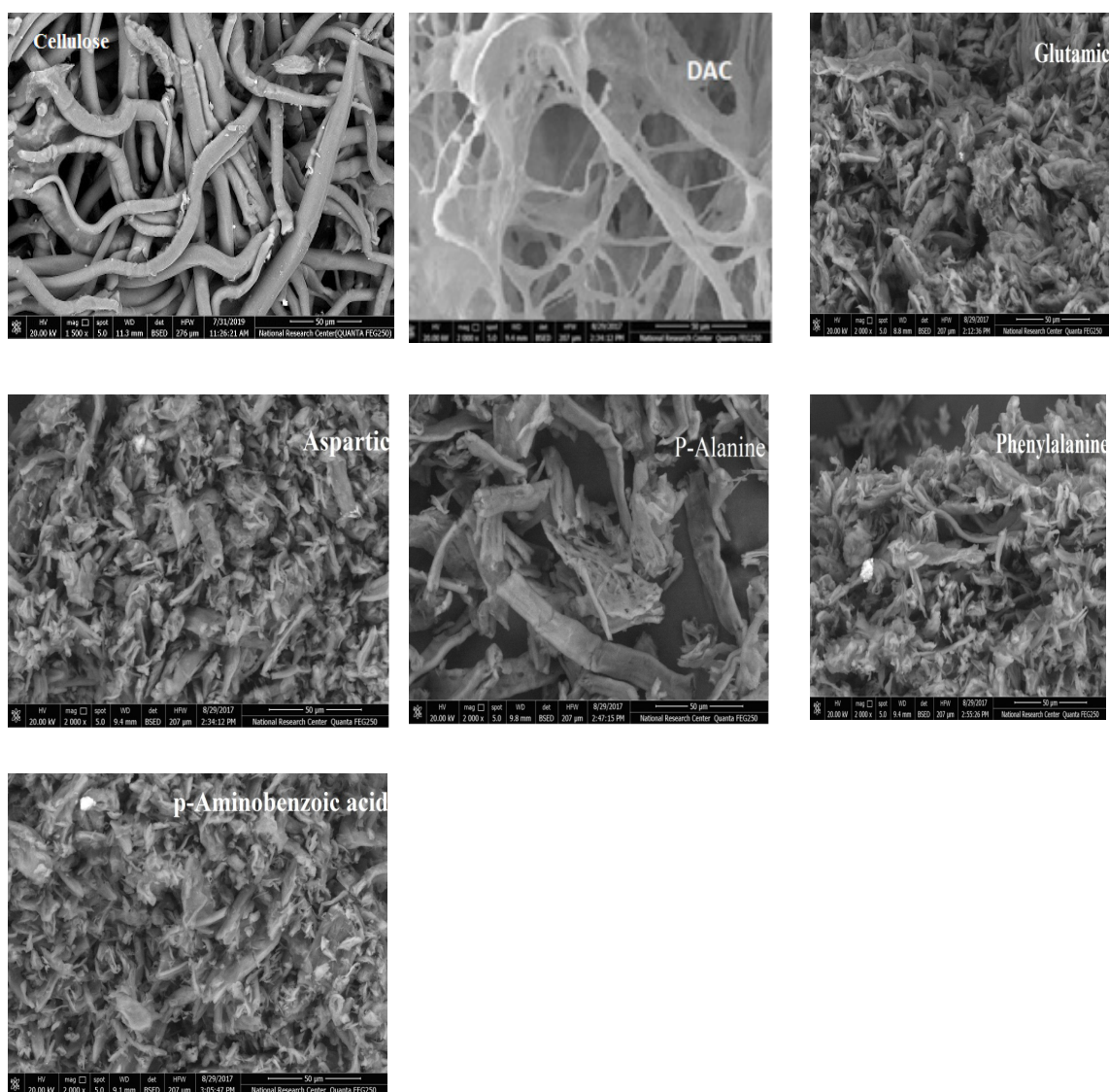


Fig. 5. SEM of Cellulose, DAC and amino acids-cellulose derivatives.

Thermogravimetric analysis

TGA is an important unique tool for evaluation and studying the thermal characteristics of polymers. In this study, the thermogravimetric experiments of the cellulose, DAC, and amino acids-DAC derivatives were performed.

Cellulose thermal decomposition process could be classified into two major reaction zones.

In the first zone (at 60.67 °C), the weight loss (average 4.861%) mainly was due to vaporization of the bounded hydrated water in the pores system of the internal surface area that belongs to supermolecular cellulosic structure. This leads to additional chain scissions, but maintains the 1,4 polysaccharide skeleton. In the second zone (up to 353.34 °C), the weight loss (average 75.54%) is attributed to progression of cellulose degradation as dehydration, depolymerization and decomposition of cellulose glucosyl units afterward the charred residue was formed.

The thermal decomposition curve of oxidized cellulose could be divided to three main reaction zones. There is weight loss (average 17.15%), showed in the first Zone (up to 65.67°C), it is mainly attributed to vaporization of the hydrated water and the low-molecular weight component in the cellulosic structure. This leads to additional chain scissions, but maintains the 1,4 polysaccharide skeleton.

In the second zone (up to 217.89°C), the weight loss (average 50.11%) is due to decomposition associated with intermolecular hemiacetal formation involving the water molecules and the aldehyde in DAC molecule, resulting in a more temperature-stable product. In the third zone (up to 327.40°C), the weight loss (average 32.17%) is due to decomposition of the carbonaceous residues [29]. The carbonaceous residue observed for DAC derivatives at ~600°C were less than 1%.

TGA was used to investigate thermal stability of amino acids functionalized 2,3-dialdehyde cellulose as was obtained from the curves depicted in Fig. 7. All TGA curves are quite similar for all prepared samples in terms of their general shape and observed degradation steps, but the step heights and the transition temperatures are different. The primary weight loss starting from room temperature up to 220°C (8%) was due to the removal of low molecular mass compounds, mostly bounded and adsorbed water. The second weight loss was detected between 310 and 370°C can be associated with neat cellulose and amino acids decomposition. These events could be accompanied with a cellulose degradation process such as dehydration, depolymerization, rearrangement, formation of carboxyl and carbonyl groups, evolution of CO₂ and CO and breakdown of glucosyl units, afterward the charred residue was formed. This stage is known as volatilization or decomposition stage [30].

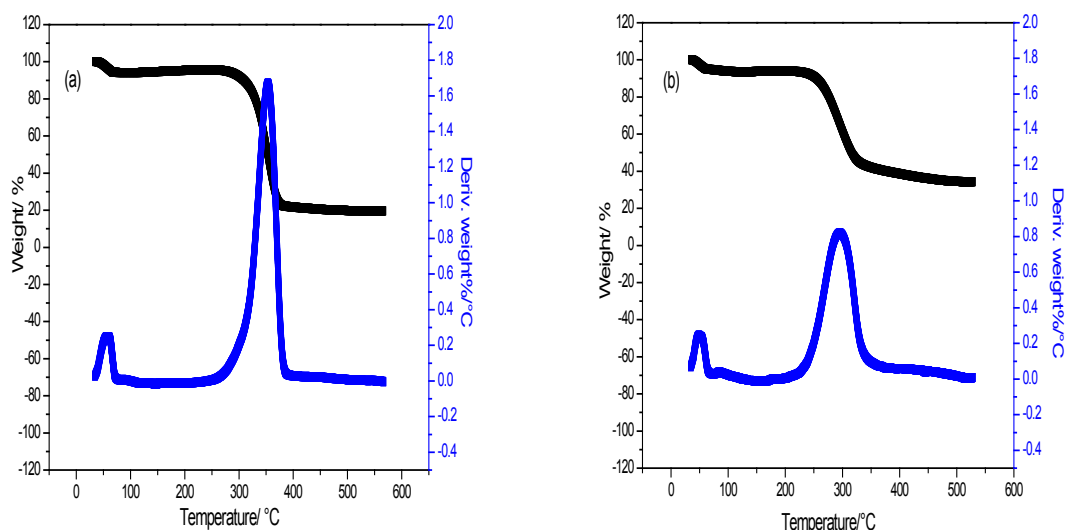


Fig. 6. TGA and DSC of cellulose and DAC

It can be seen that degradation of DAC, and its amino acids derivatives, was initiated at a lower temperature compared to that of original cellulose, which indicates that cellulose thermal stability decreases after oxidation and amino acids modification. The high thermal stability of cellulose is due to inter and intra molecular H-bonds between cellulose fibers in contrast to DAC which disordered by modification reaction. Also, the bonding energy of aldehyde was smaller and simply broken to produce minute molecules by thermal degradation. These small molecules leave the system quickly and cause quick weight loss in the system.

The incorporation of amino acid, have improved the thermal stability of the DAC by 4–22°C. This due to the formation of Schiff's base cross-linking between the amino groups of the amino acid and the aldehyde groups in DAC as well as the more stable side chain and/or aromatic ring structure involved in the polymer.

It is known that, cellulose is more stable than its amino acids derivatives, since the formation of unsaturated C-N bonds in the Schiff base causes easier formation of volatile material from the molecule.

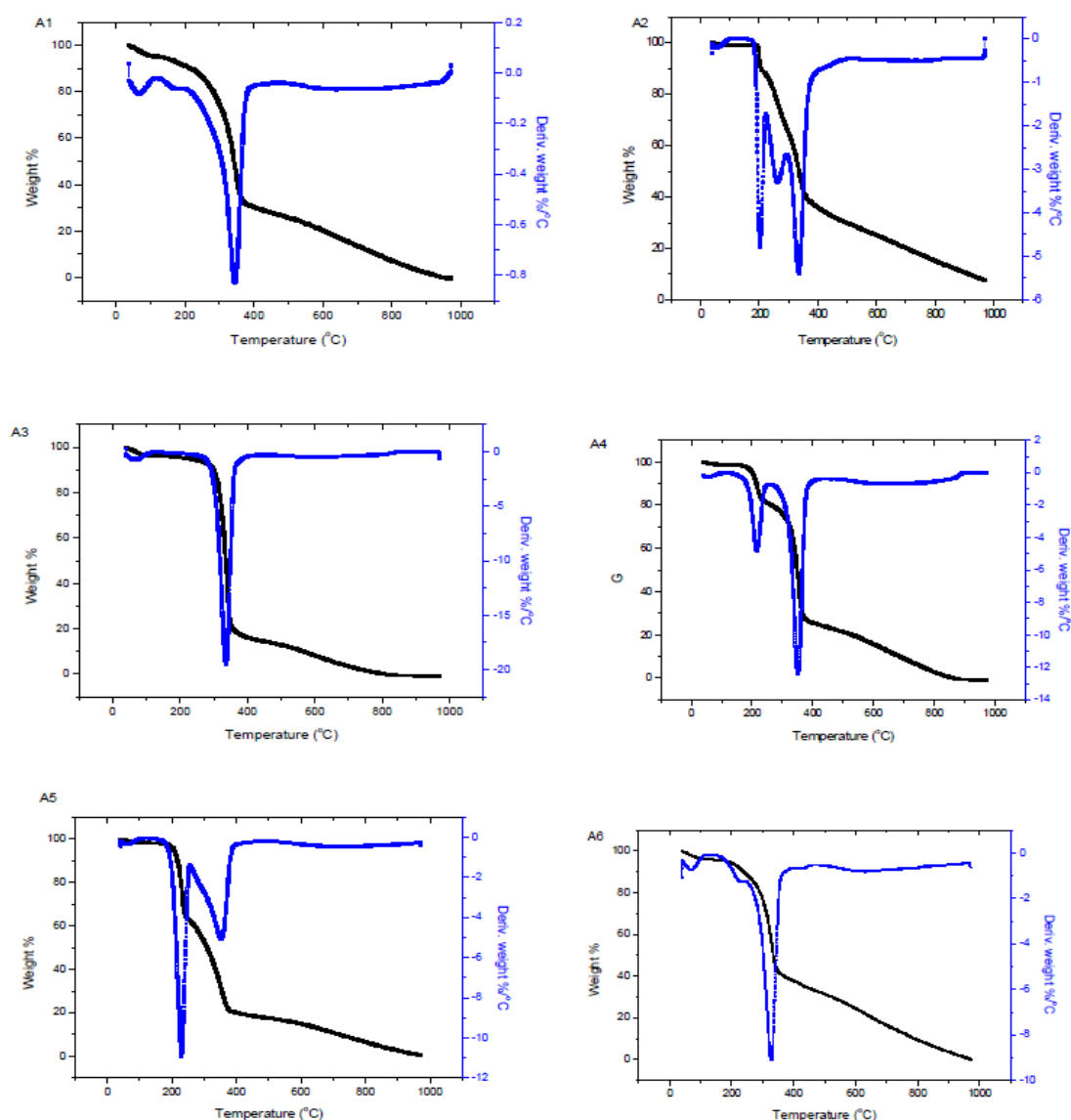


Fig. 7. TGA and DSC of amino acids-cellulose derivatives A1) Lysine, A2) Glutamic acid, A3) Aspartic acid, A4) β -Alanine, A5) Phenylalanine, A6) *p*-Aminobenzoic acid.

CP/MAS ¹³C-NMR Analysis of Cellulose

NMR has been used as a reliable tool to elucidate the chemical and physical properties of polymers.

The CP/MAS ¹³C-NMR spectra of the Cellulose, DAC, and amino acids derivatives are shown in Figure 8. As shown, Figure 8 displayed five characteristic signals of the starting cellulose at 66.7, 76.8, 78.1, 108.9, 163.1 and 163.5 ppm attributed to Cell-C6, Cell-C4, Cell-C5, Cell-1, Cell-C3 and Cell-C2, respectively [31]. The strong overlapping absorption signal at 74.61 ppm was due to the crystalline and noncrystalline area of C2, C3, and C5 on the glucose unit of cellulose.

CP/MAS ¹³C-NMR Analysis of DAC

Figure 8, showed the lack of an obvious narrow, sharp crystallization peak in DAC which refers to the destruction of crystallization zone of cellulose after oxidation. Due to the presence of aldehyde in the oxidized cellulose, the carbons C1, C4, and C6 had different shifts with the values of 101.32, 92.89 and the small wide peak around 66.8 ppm, respectively. The absorption peaks at 73.06 ppm clarifies the regular overlapping of C5 with the hydroxyl oxidation of C2 and C3 and the hydroxyl nonoxidation of C2 and C3 in DAC.

The expected absence of a carbonyl signal at 175–172 ppm proves the hemiacetal linkages formation between the aldehyde groups in DAC. In summary, studied DAC solution is mainly composed from C6-bonded hemiacetals. This was expected, because most of C2 and C3 hydroxyl groups were converted to aldehyde groups in oxidized DAC.

CP/MAS ¹³C-NMR Analysis of DAC amino acids derivatives

For the ¹³C-NMR spectrum of DAC-amino acids (Figure 9), the overlapping peaks of C2 and C3 with C5 made it difficult to analyze the chemical shift alterations of C2 and C3. Although the C1, C4 and C6 chemical shifts have overlapped quite little, and also the cellulose molecules had no free carbonyl positions in the C1 and C4, but the chemical shifts of C1 and C4 definitely changed due to the adjacency of C2, C3 and C1, C4. The chemical shift of C1 deviated to a low field was 98 ppm while the C4 position in the high field was 74 ppm. The absorption peak of C2, C3, and C5 also shifted to 79 ppm. At the low field, C6 chemical shift was appeared at 65 ppm as two divided weak peaks, this because of the Schiff base reaction of the amino acids and DAC forming azomethine group [32].

Conclusion

Starting from bagasse, alpha-cellulose was extracted and oxidized by periodate to dialdehyde cellulose (DAC). Schiff base reaction of DAC with amino acids was performed and elucidated by different analyses techniques. Results prove the successful formation of Schiff base with several amino acids in adequate degree of substitution. Optimization of the reaction condition with a specific amino acid by adapted method (as protected amino acid) to get a satisfactory degree of substitution proper to a vital application (as metal ion/dyes removal or potential biomedical applications) is under consideration for the next part of this study.

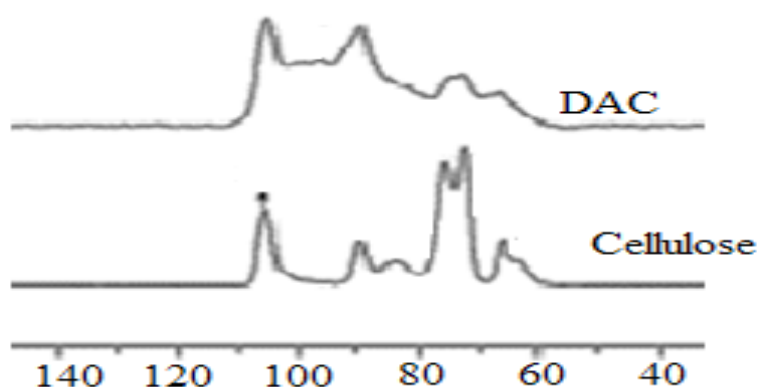


Fig. 8. Solid state ¹³C NMR for Cellulose and DAC.

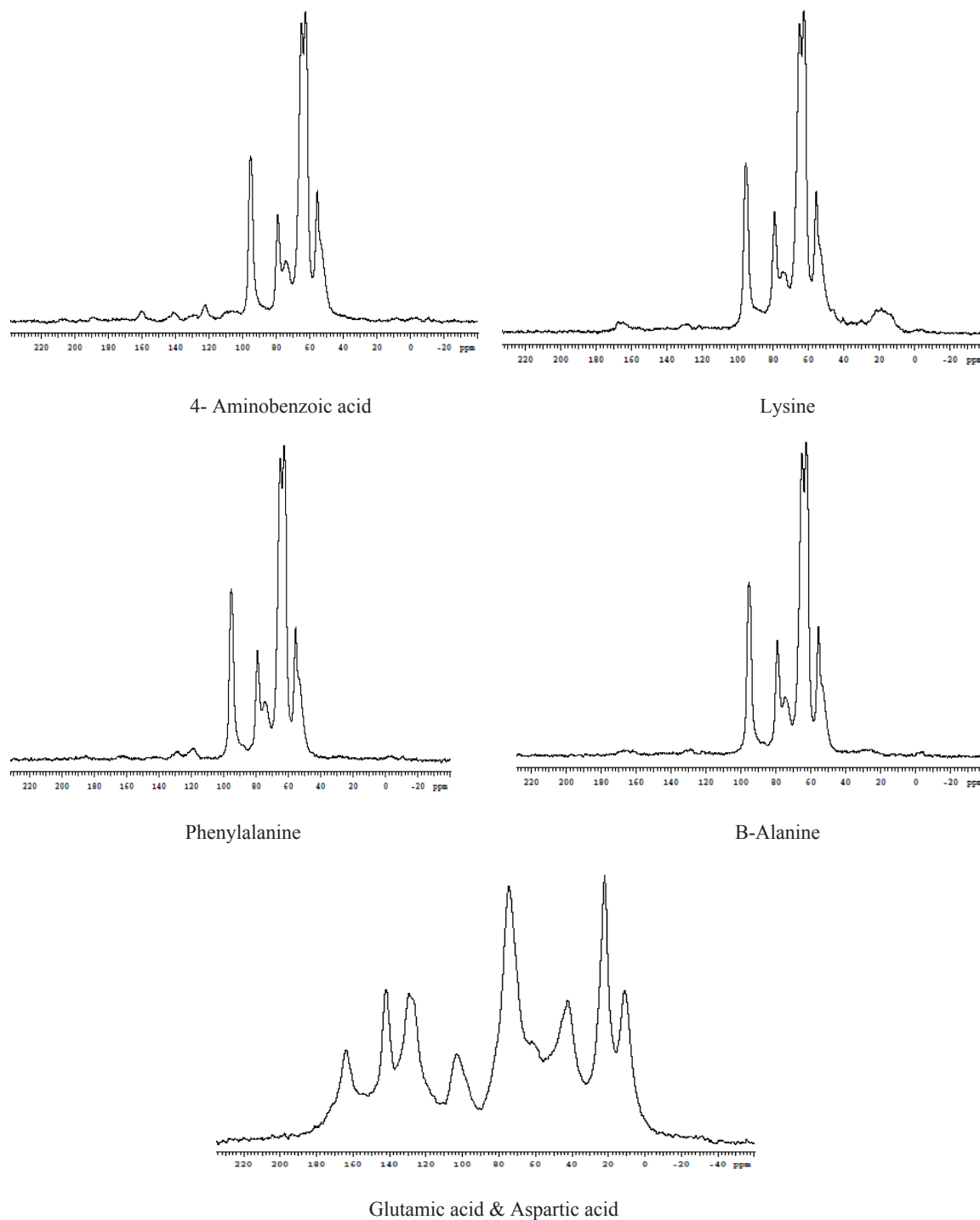


Fig. 9. Solid state ^{13}C NMR for amino acids-cellulose derivatives.

Conflict of Interests

The authors declare that they have no conflict to interests.

Acknowledgement

The authors acknowledge the National Research Centre, Egypt and Institut francais

Egypt.J.Chem. **63**, No. 9 (2020)

d’Egypte for financial support of the research activities

References

1. Fahmy Y., Fahmy T.Y.A., Mobarak F., El-Sakhawy M., Fadl M. H., Agricultural Residues (Wastes) for Manufacture of Paper, Board, and Miscellaneous

- Products: Background Overview and Future Prospects. *International Journal of ChemTech Research*, **10**(2), 424-448 (2017).
- Salama A., Etri S., Mohamed S. A. and El-Sakhawy M., Carboxymethyl cellulose prepared from mesquite tree: New source for promising nanocomposite materials. *Carbohydrate polymers*, **189**, 138-144 (2018).
 - Salama A., Shukry N., El-Gendy A. and El-Sakhawy M., Bioactive cellulose grafted soy protein isolate towards biomimetic calcium phosphate mineralization. *Industrial crops and products*, **95**, 170-174 (2017).
 - Ogiwara T., Katsumura A., Sugimura K., Teramoto Y., and Nishio, Y., Calcium phosphate mineralization in cellulose derivative/poly (acrylic acid) composites having a chiral nematic mesomorphic structure. *Biomacromolecules*, **16**(12), 3959-3969 (2015).
 - Salama A., and El-Sakhawy M., Regenerated cellulose/wool blend enhanced biomimetic hydroxyapatite mineralization. *International journal of biological macromolecules*, **92**, 920-925 (2016).
 - Tang J., Sisler J., Grishkewich N., and Tam K. C., Functionalization of cellulose nanocrystals for advanced applications. *Journal of colloid and interface science*, **494**, 397-409 (2017).
 - Varma A. J. and Kulkarni, M. P., Oxidation of cellulose under controlled conditions. *Polymer Degradation and Stability*, **77**(1), 25-27 (2002).
 - Ruan C., Strømme M., and Lindh J., A green and simple method for preparation of an efficient palladium adsorbent based on cysteine functionalized 2, 3-dialdehyde cellulose. *Cellulose*, **23**(4), 2627-2638 (2016).
 - Gruner S. A., Locardi E., Lohof E. and Kessler, H., Carbohydrate-based mimetics in drug design: sugar amino acids and carbohydrate scaffolds. *Chemical reviews*, **102**(2), 491-514 (2002).
 - Kumari S. and Chauhan G. S., New cellulose-lysine schiff-base-based sensor-adsorbent for mercury ions. *ACS applied materials and interfaces*, **6**(8), 5908-5917 (2014).
 - El-Sakhawy M., Kamel S., Salama A., Youssef M. A., Elsaid W. and Tohamy H., Amphiphilic cellulose as stabilizer for oil/water emulsion. *Egyptian Journal of Chemistry*, **60**(2), 181-204 (2017).
 - Naglah A. M., Al-Omar M. A., Kalmouch A., Gobouri A. A., Abdel-Hafez S. H., El-Megharbel S. M., and Refat M. S., Synthesis, Spectroscopy, and Anticancer Activity of Two New Nanoscale Au (III) N 4 Schiff Base Complexes. *Russian Journal of General Chemistry*, **89**(8), 1702-1706 (2019).
 - Naglah A., Ahmed A., Wen Z. H., Al-Omar M., Amr A. and Kalmouch A., New inducible nitric oxide synthase and cyclooxygenase-2 inhibitors, nalidixic acid linked to isatin schiff bases via certain L-amino acid bridges. *Molecules*, **21**(4), 498 (2016).
 - El-Menshaway A. M., Salama A. and El-Asmy A. A., New modified cellulose for separation and determination of mercury in environmental water samples. *Canadian Journal of Analytical Sciences and Spectroscopy*, **53**, 206-213 (2008).
 - Dash R., Elder T., and Ragauskas A. J., Grafting of model primary amine compounds to cellulose nanowhiskers through periodate oxidation. *Cellulose*, **19**(6), 2069-2079 (2012).
 - Kumari S., Mankotia D. and Chauhan G. S., Crosslinked cellulose dialdehyde for Congo red removal from its aqueous solutions. *Journal of environmental chemical engineering*, **4**(1), 1126-1136 (2016).
 - Jin L., Li W., Xu Q. and Sun Q., Amino-functionalized nanocrystalline cellulose as an adsorbent for anionic dyes. *Cellulose*, **22**(4), 2443-2456 (2015).
 - Zhang N., Zang G. L., Shi C., Yu H. Q. and Sheng G. P., A novel adsorbent TEMPO-mediated oxidized cellulose nanofibrils modified with PEI: Preparation, characterization, and application for Cu (II) removal. *Journal of hazardous materials*, **316**, 11-18 (2016).
 - Hu D., Jiang R., Wang N., Xu H., Wang Y. G. and Ouyang, X. K., Adsorption of diclofenac sodium on bilayer amino-functionalized cellulose nanocrystals/chitosan composite. *Journal of hazardous materials*, **369**, 483-493 (2019).
 - Omer A. M., Ammar Y. A., Mohamed G. A. and Tamer T. M., Preparation of Isatin/chitosan schiff base as novel antibacterial biomaterials. *Egyptian Journal of Chemistry*, **62**(Special Issue (Part 1)), 123-131 (2019).
 - Sirviö J., Liimatainen H., Niinimäki J. and Hormi O., Dialdehyde cellulose microfibers generated from wood pulp by milling-induced periodate

- oxidation. *Carbohydrate polymers*, **86**(1), 260-265 (2011).
22. Lucia A., van Herwijnen H. W., Oberlerchner J. T., Rosenau T. and Beaumont M., Resource□Saving Production of Dialdehyde Cellulose: Optimization of the Process at High Pulp Consistency. *ChemSusChem*, **12**(20), 4679-4684 (2019).
23. Eyley S. and Thielemans W., Surface modification of cellulose nanocrystals. *Nanoscale*, **6**(14), 7764-7779 (2014).
24. Plappert S. F., Quraishi S., Pircher N., Mikkonen K. S., Veigel S., Klinger K. M. and Liebner F. W., Transparent, flexible, and strong 2, 3-dialdehyde cellulose films with high oxygen barrier properties. *Biomacromolecules*, **19**(7), 2969-2978 (2018).
25. Godoy-Alcántar C., Yatsimirsky A. K. and Lehn J. M., Structure-stability correlations for imine formation in aqueous solution. *Journal of Physical Organic Chemistry*, **18**(10), 979-985 (2005).
26. El-Sakhawy M., Kamel S., Salama A. and Tohamy H. A. S., Preparation and infrared study of cellulose based amphiphilic materials. *Cellulose Chemistry and Technology*, **52**, 193-200 (2018).
27. Pietrucha K., and Safandowska M., Dialdehyde cellulose-crosslinked collagen and its physico chemical properties. *Process Biochemistry*, **50** (12), 2105-2111 (2015).
28. Kim U. J., Lee Y. R., Kang T. H., Choi J. W., Kimura S. and Wada M., Protein adsorption of dialdehyde cellulose-crosslinked chitosan with high amino group contents. *Carbohydrate polymers*, **163**, 34-42 (2017).
29. El-Sakhawy M., Nashy E. S. H., El-Gendy A. and Kamel S., Thermal and natural aging of bagasse paper sheets coated with gelatin. *Nordic Pulp and Paper Research Journal*, **33**(2), 327-335 (2018).
30. El-Sakhawy M., Tohamy H. A. S., Salama A. and Kamel S., Thermal properties of carboxymethyl cellulose acetate butyrate. *Cellulose Chemistry and Technology*, **53**(7-8), 667-675 (2019).
31. Kono H., Yunoki S., Shikano T., Fujiwara M., Erata T. and Takai M., CP/MAS 13C NMR study of cellulose and cellulose derivatives. 1. Complete assignment of the CP/MAS 13C NMR spectrum of the native cellulose. *Journal of the American Chemical Society*, **124**(25), 7506-7511 (2002).
32. George D., Maheswari P. U. and Begum K. M. S., Cysteine conjugated chitosan based green nanohybrid hydrogel embedded with zinc oxide nanoparticles towards enhanced therapeutic potential of naringenin. *Reactive and Functional Polymers*, **148**, 104480 (2020).